



AFRL-RY-WP-TR-2021-0181

**A CRITICAL ASSESSMENT OF ELECTRON
TRANSPORT THEORY**

**Evaluation of Electron Scattering by Ionized Impurities –
Phase 1**

**Daniel L. Rode
Pendragon Associates**

**AUGUST 2021
Final Report**

**DISTRIBUTION STATEMENT A. Approved for public release. Distribution is unlimited.
*See additional restrictions described on inside pages***

STINFO COPY

**AIR FORCE RESEARCH LABORATORY
SENSORS DIRECTORATE
WRIGHT-PATTERSON AIR FORCE BASE, OH 45433-7320
AIR FORCE MATERIEL COMMAND
UNITED STATES AIR FORCE**

NOTICE AND SIGNATURE PAGE

Using Government drawings, specifications, or other data included in this document for any purpose other than Government procurement does not in any way obligate the U.S. Government. The fact that the Government formulated or supplied the drawings, specifications, or other data does not license the holder or any other person or corporation; or convey any rights or permission to manufacture, use, or sell any patented invention that may relate to them.

This report was cleared for public release by the USAF 88th Air Base Wing (88 ABW) Public Affairs Office (PAO) and is available to the general public, including foreign nationals. Copies may be obtained from the Defense Technical Information Center (DTIC) (<http://www.dtic.mil>).

AFRL-RY-WP-TR-2021-0181 HAS BEEN REVIEWED AND IS APPROVED FOR PUBLICATION IN ACCORDANCE WITH ASSIGNED DISTRIBUTION STATEMENT.

**/Signature/*

JOHN S. CETNAR
Program Manager
Electronic Devices Branch
Aerospace Components & Subsystems Division

**/Signature/*

ROSS W. DETTMER, Chief
Electronic Devices Branch
Aerospace Components & Subsystems

**/Signature/*

LESTER C. LONG, Lt Col, USAF
Deputy
Aerospace Components & Subsystems Division
Sensors Directorate

This report is published in the interest of scientific and technical information exchange, and its publication does not constitute the Government's approval or disapproval of its ideas or findings.

Disseminated copies will show “/Signature/” stamped or typed above the signature blocks.

REPORT DOCUMENTATION PAGE				<i>Form Approved</i> OMB No. 0704-0188	
<p>The public reporting burden for this collection of information is estimated to average 1 hour per response, including the time for reviewing instructions, searching existing data sources, gathering and maintaining the data needed, and completing and reviewing the collection of information. Send comments regarding this burden estimate or any other aspect of this collection of information, including suggestions for reducing this burden, to Department of Defense, Washington Headquarters Services, Directorate for Information Operations and Reports (0704-0188), 1215 Jefferson Davis Highway, Suite 1204, Arlington, VA 22202-4302. Respondents should be aware that notwithstanding any other provision of law, no person shall be subject to any penalty for failing to comply with a collection of information if it does not display a currently valid OMB control number. PLEASE DO NOT RETURN YOUR FORM TO THE ABOVE ADDRESS.</p>					
1. REPORT DATE (DD-MM-YY) August 2021		2. REPORT TYPE Final		3. DATES COVERED (From - To) 1 November 2020 – 1 November 2020	
4. TITLE AND SUBTITLE A CRITICAL ASSESSMENT OF ELECTRON TRANSPORT THEORY Evaluation of Electron Scattering by Ionized Impurities – Phase 1				5a. CONTRACT NUMBER FA9550-20RXCOR046-RY	
				5b. GRANT NUMBER	
				5c. PROGRAM ELEMENT NUMBER N/A	
6. AUTHOR(S) Daniel L. Rode				5d. PROJECT NUMBER N/A	
				5e. TASK NUMBER N/A	
				5f. WORK UNIT NUMBER N/A	
7. PERFORMING ORGANIZATION NAME(S) AND ADDRESS(ES) Pendragon Associates 16400 Collins Avenue, Unit 2846 Sunny Isles Beach, Florida 33160				8. PERFORMING ORGANIZATION REPORT NUMBER	
9. SPONSORING/MONITORING AGENCY NAME(S) AND ADDRESS(ES) Air Force Research Laboratory Sensors Directorate Wright-Patterson Air Force Base, OH 45433-7320 Air Force Materiel Command United States Air Force				10. SPONSORING/MONITORING AGENCY ACRONYM(S) AFRL/Rydd	
				11. SPONSORING/MONITORING AGENCY REPORT NUMBER(S) AFRL-RY-WP-TR-2021-0181	
12. DISTRIBUTION/AVAILABILITY STATEMENT DISTRIBUTION STATEMENT A. Approved for public release. Distribution is unlimited.					
13. SUPPLEMENTARY NOTES PAO case number AFRL-2021-0824, Clearance Date 11 March 2021. Report contains color.					
14. ABSTRACT The present work is directed toward a critical examination of the current state-of-the-art of the theory of electron transport in semiconductors. In the case of undoped semiconductors and their alloys, theory agrees with experiment within a few percent and current theory can be accepted as being truly established. In the case of doped semiconductors, a distinction must be made between two regimes, nondegenerate and degenerate doping (or lightly doped and heavily doped). Degeneracy may be brought on either by large concentrations of dopant impurities, or by sufficiently low temperatures, or both. In the case of nondegenerate semiconductors, theory agrees with experiment within a few percent and the theory can be regarded as being sufficient for most purposes. For degenerate semiconductors, several experimental studies clearly indicate significant deficiencies in the current theory. These works call into question the validity of the widely used Brooks-Herring theory of electron scattering by ionized impurities. The BH theory is critically examined and serious shortcomings are pointed out. A different theory of ionized impurity scattering by Falicov and Cuevas is discussed as a possible alternative. But, this too appears not to be entirely acceptable. Nevertheless, it does suggest a viable alternative approach to an accurate description of doped semiconductors, which will be the subject of Phase 2 of the present work.					
15. SUBJECT TERMS degeneracy, electron mobility, electronic transport, semiconductor(s)					
16. SECURITY CLASSIFICATION OF:			17. LIMITATION OF ABSTRACT: SAR	8. NUMBER OF PAGES 25	19a. NAME OF RESPONSIBLE PERSON (Monitor) John Cetnar
a. REPORT Unclassified	b. ABSTRACT Unclassified	c. THIS PAGE Unclassified			

Table of Contents

Section	Page
List of Figures	ii
1 PHASE 1: A CRITICAL ASSESSMENT OF ELECTRON TRANSPORT THEORY	1
1.1 What Is the Status of Electron Transport Theory in Semiconductors?.....	1
1.2 Electron Transport in Pure and Lightly Doped Semiconductors	1
1.3 Electron Transport in More Heavily Doped Semiconductors	5
1.4 Brooks-Herring and Falicov-Cuevas Theories of Ionized-Impurity Scattering	9
1.5 When Do the Brooks-Herring and Falicov-Cuevas Theories Diverge?	12
1.6 Comparisons between BH and FC Theories.....	13
2 CONCLUSION	15
3 ACKNOWLEDGMENTS	16
APPENDIX	17
4 REFERENCES	18
LIST OF SYMBOLS, ABBREVIATIONS, AND ACRONYMS	20

List of Figures

Figure	Page
Figure 1: Electron Mobility of High-purity Ge Calculated Using SETA	3
Figure 2: Electron Mobility of High-purity CdS Calculated using SETA.....	4
Figure 3: Electron Mobility of Lightly Doped GaAs Calculated Using SETA	5
Figure 4: 300K Electron Mobility of Doped GaAs Compiled by Sotoodeh ⁸ and by Stillman ⁹ <i>et al</i>	6
300K GaAs	6
Figure 5: 300K Hall Factors of Doped GaAs Calculated by SETA.....	6
Figure 6: 300K Electron Mobility of Doped GaAs Compiled by Sotoodeh ⁸ and by Stillman ⁹ <i>et al</i>	7
Figure 7: Same Results as Figure 6 for only the Heavily Doped Region, Showing Strong Disagreement between Experiment and Theory using the BH Theory	8
Figure 8: The Experimental 77K Hall Mobility of Electrons in LPE-grown InP is shown as Data Points	8
Figure 9: Same samples as Figure 8 but for 300K	9
Figure 10: Electron Mobility of High-purity Ge in Deep Freeze-out (experiment curve <i>a</i>). Mobility Vanishes at $T = 0K$. The BH Mobility (curve <i>b</i>) diverges at $T = 0K$	11
Figure 11: 300K Electron Mobility of Doped GaAs Compiled by Sotoodeh ⁸ and by Stillman ⁹ <i>et al</i>	14
Figure 12: 77K Electron Mobility of Doped GaAs by Balk ¹⁰ and by Kuphal ¹¹ Compared to BH Theory (dashed curve) and FC Theory (solid curves)	14

1 PHASE 1: A CRITICAL ASSESSMENT OF ELECTRON TRANSPORT THEORY

By Daniel L. Rode
Pendragon Associates

1.1 What Is the Status of Electron Transport Theory in Semiconductors?

That is the question. The present work is directed toward a critical examination of the current state-of-the-art of the theory of electron transport in semiconductors.¹ The answer can be broken into two general parts:

- a) electron transport in pure, undoped semiconductors, and
- b) electron transport in doped semiconductors

In the case of pure, undoped semiconductors and their alloys, electron mobility (which is the fundamental measure of electron transport) is determined by lattice scattering due to deformation potential acoustic and piezoelectric acoustic phonons, by polar and nonpolar optical phonons, and due to alloy scattering.^{2,3} In these cases, theory agrees with experiment within a few percent and current theory can be accepted as being truly established. See Sec. II below.

In the case of doped semiconductors, a distinction must be made between two regimes — nondegenerate and degenerate doping (or lightly doped and heavily doped). Degeneracy may be brought on either by large concentrations of dopant impurities, or by sufficiently low temperatures, or both. In the case of nondegenerate semiconductors that are lightly doped, theory agrees with experiment within a few percent and the theory can be regarded as being sufficient for most purposes. See Sec. III below.

On the other hand, as doping concentration is increased, there are several experimental studies that clearly indicate significant deficiencies in the current theory. These works call into question the validity of the widely used Brooks-Herring (BH) theory of electron scattering by ionized impurities (hereafter BH).⁴ In Sec. IV below, the BH theory is critically examined and serious shortcomings are pointed out. A different theory of ionized impurity scattering by Falicov and Cuevas (hereafter FC) is discussed as a possible alternative, although this too appears not to be entirely acceptable.⁵ Nevertheless, it does suggest a viable alternative approach to an accurate description of doped semiconductors, which will be the subject of Phase 2 of the present work.

1.2 Electron Transport in Pure and Lightly Doped Semiconductors

In the following, theoretical calculations of electron transport properties are carried out using the Fortran computer program semiconductor electronic transport analysis (SETA). SETA incorporates nonparabolic bands, wave function admixture, and electron degeneracy without approximation. Electron scattering includes piezoelectric acoustic phonons, deformation potential acoustic phonons, and polar and nonpolar phonons for direct-gap

materials, and in addition intervalley phonons for indirect-gap semiconductors with multiple conduction-band minima. The computations are carried out using iterations of contraction mappings, which ensures uniqueness and convergence of the numerical solutions. All of the galvanomagnetic and thermoelectric transport coefficients are calculated, including:

- Fermi level: E_F
- Electron drift mobility: μ
- Electron Hall mobility in the magnetic field $B = 0$ limit: μ_H
- Electron Hall mobility for arbitrary finite, classical B : μ_B
- Short sample magnetoresistance: μ_S
- Long sample magnetoresistance: μ_L
- Thermoelectric coefficient: Q

Theoretical and experimental results are shown to agree within a few percent for pure and low-doped semiconductors, as shown in Figures 1, 2, and 3 for Ge, CdS, and GaAs.^{2, 6} In the first two cases, mobility is entirely determined by so-called lattice scattering.

There is no significant ionized-impurity scattering. In the third case (GaAs), below 100K ionized impurity scattering becomes progressively more important and is included using the Brooks-Herring treatment with good success.

In the case of Ge in Figure 1, there are two adjustable parameters, which set the strengths of nonpolar optical phonon scattering above 80K and acoustic phonon scattering below 60K, respectively. Ge possesses cubic symmetry (diamond structure) and mobility is independent of sample orientation. Note that the drift mobility reaches well over one million. Despite the use of these two adjustable material parameters, the accuracy of the comparison strongly suggests that the fundamental description of electron transport is correct, leaving little more to be desired in this case.

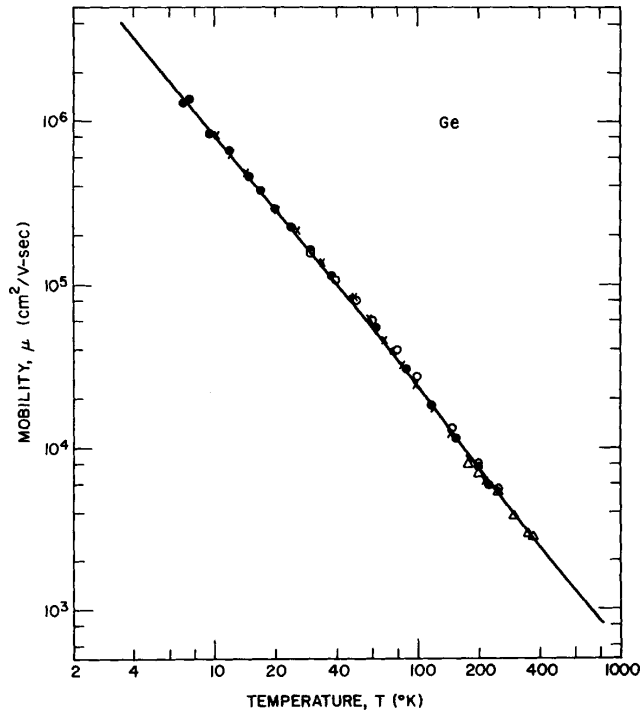


Figure 1: Electron Mobility of High-purity Ge Calculated Using SETA Curve

In the case of CdS in Figure 2, there are no adjustable parameters, all of the material parameters having been previously determined by direct measurement independent of transport properties. This is the ideal case and is to be striven for. The drift mobility is dominated by polar optical phonons above 80K and by piezoelectric phonons below 60K. CdS possesses hexagonal symmetry (wurtzite structure) and can be characterized using electrical current flow either parallel or transverse to the c-axis, as indicated. The accuracy of the comparison is satisfactory for the higher temperatures, but the results below 60K suggest that the measurements of the piezoelectric coefficients need to be revisited. Good agreement between theory and experiment for piezoelectric scattering for other materials indicates that the error lies not on the theoretical side.

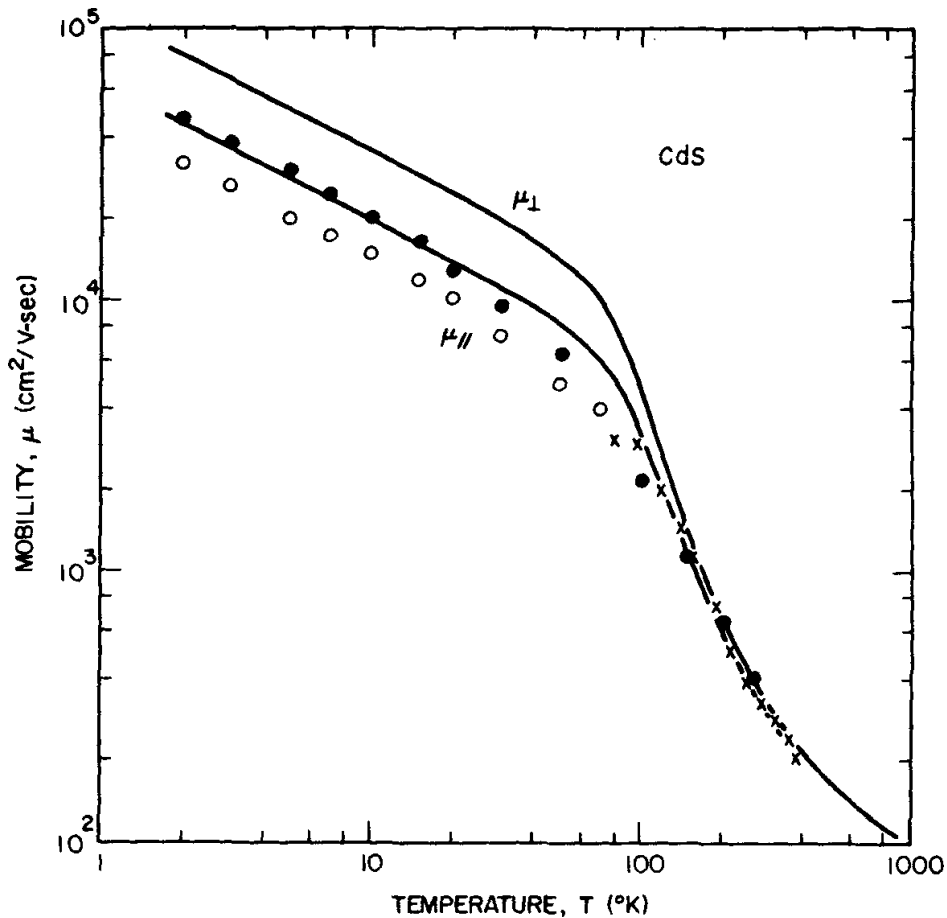


Figure 2: Electron Mobility of High-purity CdS Calculated using SETA Curve

For the GaAs sample shown in Figure 3 there is only one adjustable parameter, the ionized acceptor concentration N_A . See the Appendix and Rode² for material parameters. Here, the distinction between drift mobility and finite B Hall mobility is emphasized.

The 5kG Hall mobility is dominated by polar optical phonons above 100K and by ionized impurity scattering below 40K. In between, both deformation potential acoustic and piezoelectric acoustic scattering are important. GaAs possesses cubic symmetry (zincblende structure) and mobility is independent of sample orientation. The accuracy of the comparison is quite satisfactory over the entire range of temperatures shown.

It is important to note that ionized impurity scattering here is described by use of the BH theory. This matter will be examined carefully in the following sections.

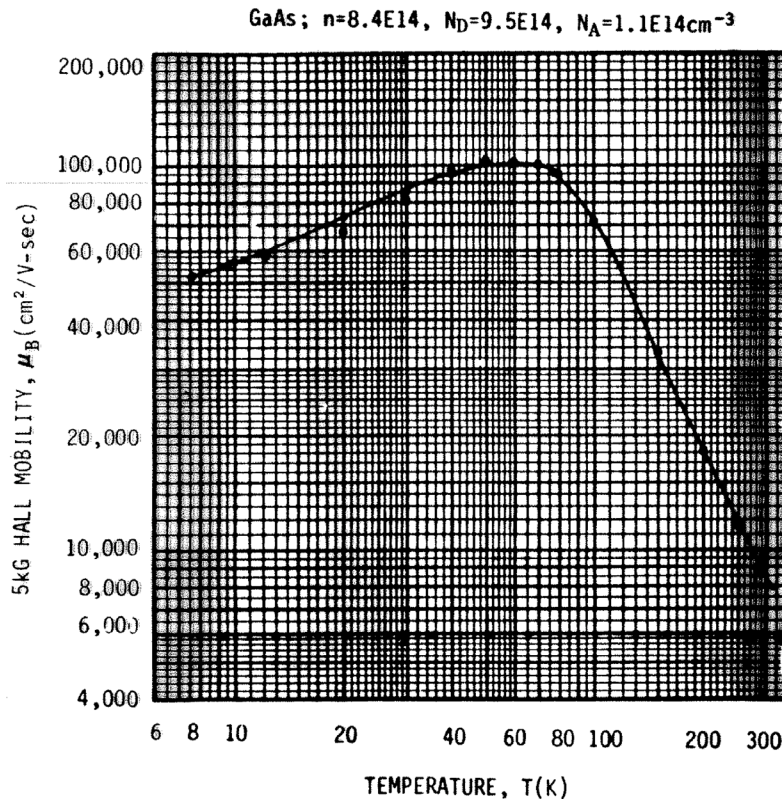


Figure 3: Electron Mobility of Lightly Doped GaAs Calculated Using SETA Curve

Thus, we conclude that the theory of electron transport is properly established within a few percent accuracy for both pure and for moderately doped semiconductors.⁷

1.3 Electron Transport in More Heavily Doped Semiconductors

Let us now turn to doped semiconductors. There are large quantities of data available for GaAs and for InP because of widespread interest in their commercial use. Consider room-temperature GaAs, *i.e.* 300K GaAs. Figure 4 shows compilations of data by Sotoodeh⁸ and by Stillman⁹ for 300K GaAs. Each set of these data is based on a much larger set of underlying experimental points (which to avoid prolixity are not shown) and show considerably more scatter to the extent of approximately 10% about the mean.

First of all, the data are labeled mobility, whereas it seems certain that they are in fact Hall mobility data. The authors do not specify the magnitude of the magnetic field. At $T=300K$, the difference between Hall and drift mobility can be substantial for low-doped material as shown by Figure 5. The Hall factor ($B = 0$ limit) and the finite-B Hall factor (at 5kG) exceed unity by 15 and 10 percent. Above the $mid-10^{16}/cc$ range, the correction is less than the 5% criterion we are concerned with presently and is of no concern for heavily doped material. The SETA results below assume a 5kG magnetic field.

As expected, the Hall mobility reaches up toward $8600\text{ cm}^2/V\text{-s}$ for pure GaAs at

300K and falls toward $1000 \text{ cm}^2/\text{V-s}$ for heavy doping.

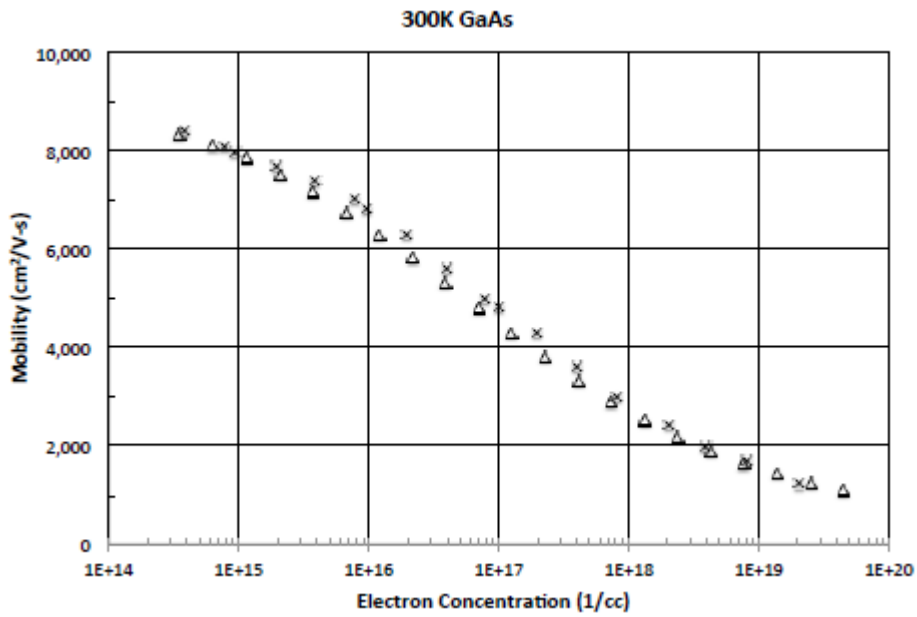


Figure 4: 300K Electron Mobility of Doped GaAs Compiled by Sotoodeh⁸ and by Stillman⁹ *et al*

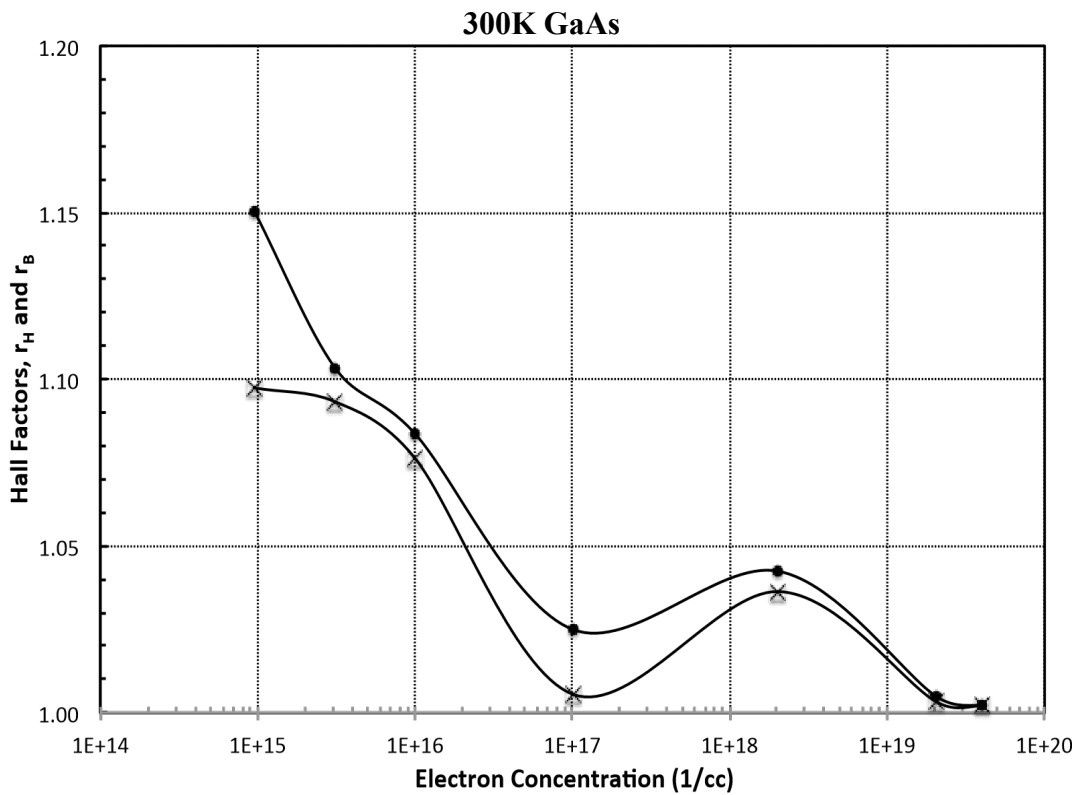


Figure 5: 300K Hall Factors of Doped GaAs Calculated by SETA Zero and 5kG

Now, consider theoretical results from SETA calculations using the BH theory of ionized impurity scattering as shown in Figure 6. Theory and experiment agree within a few percent for electron concentration below $10^{17}/\text{cc}$; better or worse agreement can be achieved by adjusting the compensating acceptor concentration but this is merely empiricism and adds little to the critical assessment. However, it is very important to note that theory and experiment disagree significantly for the larger electron concentrations, reaching as high as 43% error. This disagreement has been repeatedly pointed out by several authors for 77K GaAs, and it has been strongly suggested that it indicates a fundamental error in the theory.^{10,11,12} These arguments are further supported by experimental observations that photoluminescence does not show the presence of compensating acceptors.

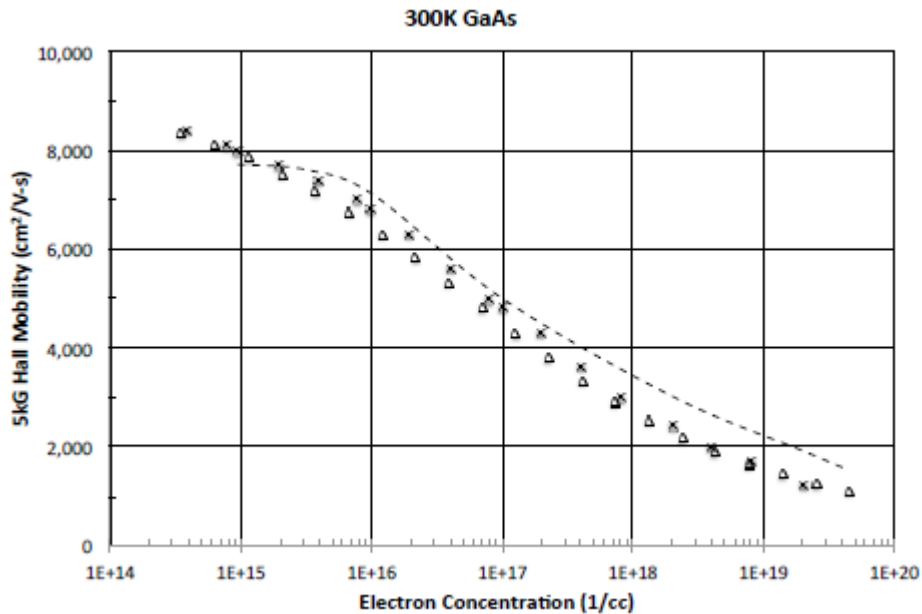


Figure 6: 300K Electron Mobility of Doped GaAs Compiled by Sotoodeh⁸ and by Stillman⁹ *et al*

Points and comparison to results calculated by SETA using the BH theory (dashed curve). The compensating acceptor concentration is arbitrarily set at $3.1 \times 10^{15}/\text{cc}$.

To emphasize this important point of disagreement, Figure 7 shows only the heavily doped region of Figure 6.

In many previous works, this disagreement has been compensated for by arbitrarily adjusting the compensating acceptor concentration. But, it will be shown below that other important factors may be at play, necessitating significant revisions away from the BH theory.

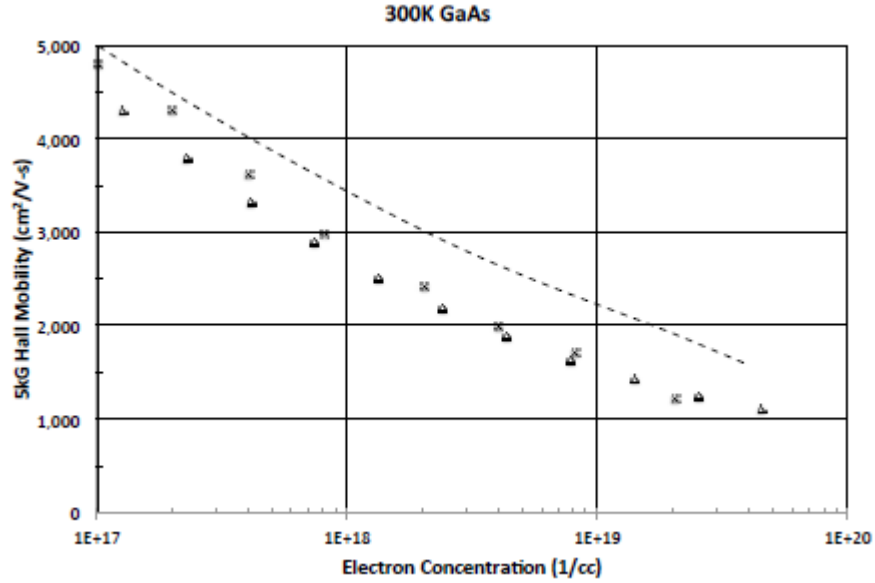


Figure 7: Same Results as Figure 6 for only the Heavily Doped Region, Showing Strong Disagreement between Experiment and Theory using the BH Theory

Now consider InP. Figure 8 shows data by Kuphal¹¹ for 77K liquid phase epitaxy (LPE) InP compared to the theoretical work of Rode and Walukiewicz based on the BH theory.

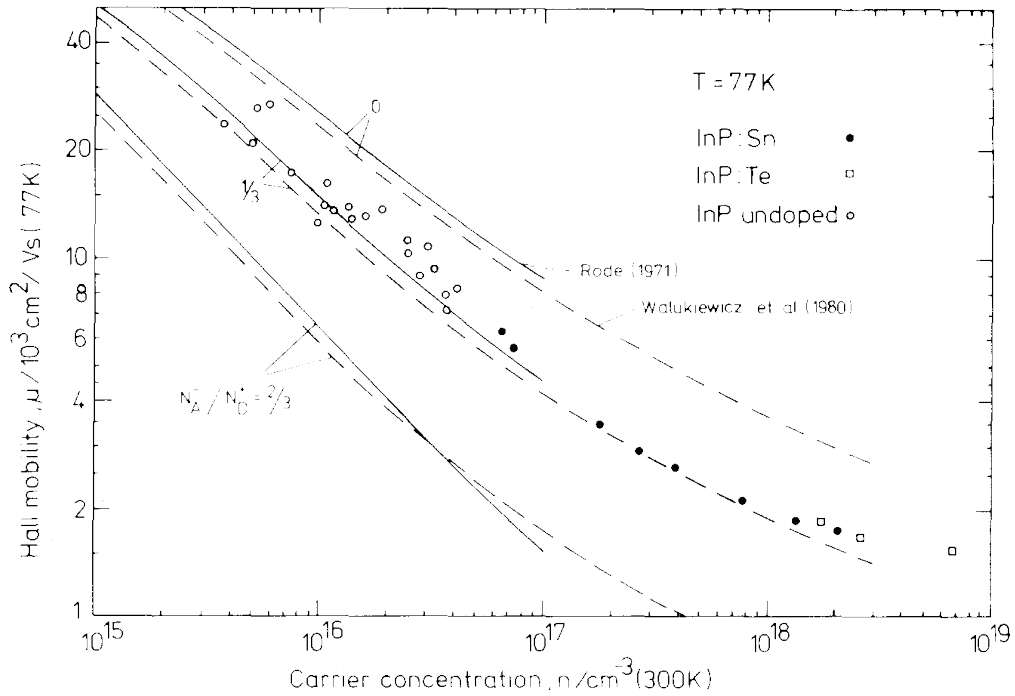


Figure 8: The Experimental 77K Hall Mobility of Electrons in LPE-grown InP is shown as Data Points

The theories of Rode and Walukiewicz (solid and dashed curves) are compared for various compensation ratios.

In Figure 8, the compensation ratio is zero, 1/3, and 2/3 for the upper, center and lower curves (acceptor/donor concentration ratios). At first, one may be inclined to interpret the data in terms of dopant compensation, but this is not tenable for two reasons:

- a) photoluminescence measurements do not reveal the implied acceptors
- b) The 300K data for these same samples suggest zero compensation (Figure 9).

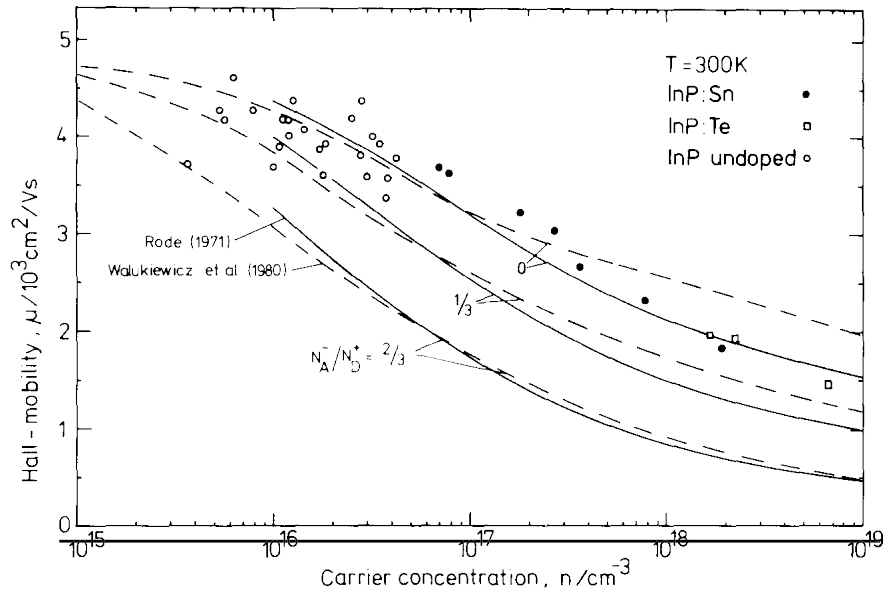


Figure 9: Same samples as Figure 8 but for 300K

It appears that the compensation ratio must be nearly zero in this case, in contradiction to the interpretation given for Figure 8.

In summary, one must conclude that dopant compensation is not the correct way to interpret the data. One is inclined to accept Anderson's suggestion¹² that the theory of electron scattering within the BH theory is incorrect when accuracy better than a factor of two, or so, is required.

1.4 Brooks-Herring and Falicov-Cuevas Theories of Ionized-Impurity Scattering

Belief in the BH theory of ionized-impurity scattering is so widespread that it is at first difficult to imagine alternatives. Nevertheless, there are hints that the BH theory is insufficient in certain cases, including heavily doped semiconductors as well as lightly doped semiconductors under deep freeze-out conditions. Consider the latter case.

Aside from a constant of multiplication, the BH scattering rate for a parabolic conduction band is given in terms of the electron momentum wave vector k and the ionized impurity screening factor β by

$$v_{ii} \approx [\ln(1 + \gamma^2) - \gamma^2 / (1 + \gamma^2)] / k^3$$

where $\gamma^2 = 4k^2 / \beta^2$

(1)

When γ is small, second-order expansion gives

$$v_{ii} \approx [\gamma^2 - \gamma^4 / 2 - \gamma^2(1 - \gamma^2)] / k^3$$

$$\approx \gamma^4 / 2k^3$$

$$\approx 8k / \beta^4$$
(2)

Clearly, the BH scattering rate (incorrectly) vanishes as momentum goes to zero, whereas it should go to infinity, as discussed below. The problem is much worse when nonparabolicity is included because the BH scattering rate may become negative in some cases. In general, the scattering rate is the product of the electron velocity v and the scattering cross-section σ . If the scattering centers are hard spheres, the cross-section is simply proportional to the squared diameter of the scattering center, *i.e.* its cross-sectional area and, hence, the scattering rate increases linearly with velocity, or momentum k . The corresponding mobility would rise to infinity at $T = 0$.

If the scattering centers are Coulomb potentials, they are not “hard” but somewhat soft and their effective diameter varies with the energy of the incoming electron, being small for large-energy electrons and large for small-energy electrons. Classically, the cross-section would vary as the reciprocal of the fourth power of the momentum because the Coulomb potential varies as $1/r$ and the electron energy varies as k^2 . So, the scattering rate would vary as $1/k^3$, giving the well-known $T^{3/2}$ dependence of ionized impurity mobility.

But here, we are interested in the small momentum case where the electron de Broglie wavelength is much greater than the screening length and $4k^2/\beta^2$ is very small. In this case, the cross-section varies as $1/k^2$ giving a scattering rate which varies as $1/k$. The mobility varies roughly linearly with k . Consequently, the mobility vanishes as the momentum approaches zero, whereas in the BH model it goes to infinity. This is clearly seen in the experimental data by Falicov and Cuevas in Figure 10.

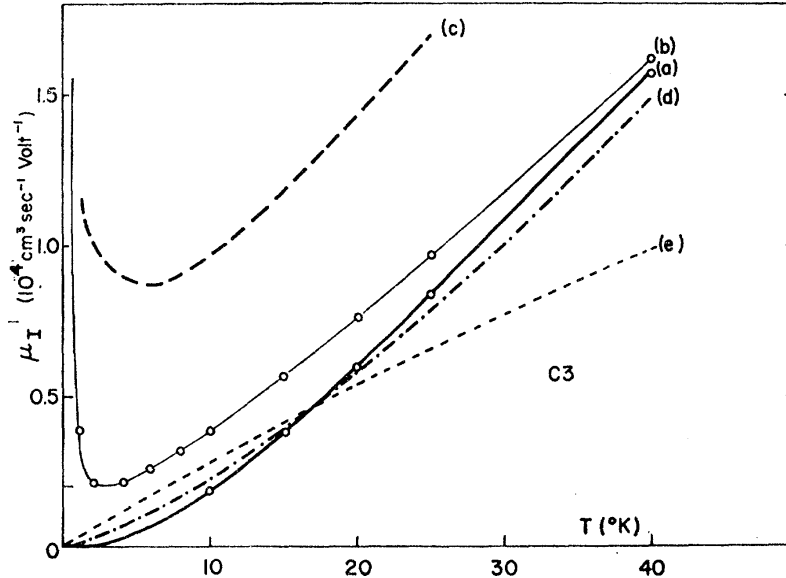


Figure 10: Electron Mobility of High-purity Ge in Deep Freeze-out (experiment curve a). Mobility Vanishes at $T = 0K$. The BH Mobility (curve b) diverges at $T = 0K$

Falicov and Cuevas go further and develop a theory of electron scattering by ionized impurities which allows for spatial correlation between donors and acceptors.⁵ The BH theory assumes the dopants are randomly distributed whereas the FC theory assumes they are exponentially correlated, as though perfect equilibrium were to obtain during crystal growth. This is a highly questionable assumption and it will be studied further in Phase 2 of this work. Meanwhile, see Fisher *et al.* for a specific counter-example for GaAs.¹⁴ Nevertheless, the FC assumption of exponential correlation serves the valuable purpose of setting an upper bound on the scattering rate, whereas the BH theory sets a lower bound. For FC scattering the scattering rate is given by

$$v_{ii} \approx [\ln(1 + \gamma^2) + \gamma^2 / (1 + \gamma^2)] / k^3 \quad (3)$$

Notice the plus sign instead of the minus sign in the BH case of equation (eq.) (1). When γ is small, second-order expansion gives

$$\begin{aligned} v_{ii} &\approx [\gamma^2 - \gamma^4 / 2 + \gamma^2(1 - \gamma^2)] / k^3 \\ &\approx 2\gamma^2 / k^3 \\ &\approx 8 / \beta^2 k \end{aligned} \quad (4)$$

The mobility varies linearly with k and it vanishes at $T = 0K$ in agreement with Figure 10. So, the FC approach solves a significant problem for the deep freeze-out case.

Below, some calculations are carried out using SETA and the FC formulation in comparison to the BH formulation. But first, one might wonder as to what conditions would cause significant differences between the FC *versus* the BH approach? This is easily answered by assuming a parabolic conduction band and a nondegenerate electron concentration in the following section.

1.5 When Do the Brooks-Herring and Falicov-Cuevas Theories Diverge?

For non-degenerate electron systems, it is easy to see that the Brooks-Herring equation is numerically almost indistinguishable from the Falicov-Cuevas equation. Consider a non-degenerate electron system and, for simplicity, a parabolic conduction band. The screened Coulomb potential of the ionized-impurity scattering centers with charge Q is

$$\varphi = \pm Qe^{-\beta r} / r \quad (5)$$

β is the screening factor, *i.e.*, the reciprocal of the screening length. The scattering rate v_{ii} due to ionized-impurities is

$$v_{ii} = Const. \times [\ln(1 + 4k^2 / \beta^2) \pm (4k^2 / \beta^2) / (1 + 4k^2 / \beta^2)] / k^3 \quad (6)$$

The minus sign represents the BH formulation and the plus sign represents the FC formulation. For convenience, define $\gamma = 2k/\beta$, so

$$v_{ii} = Const. \times [\ln(1 + \gamma^2) \pm \gamma^2 / (1 + \gamma^2)] / \gamma^3 \quad (7)$$

For a non-degenerate system of electrons

$$\beta^2 = e^2 n / \epsilon_o K \kappa T \quad (8)$$

K is the low-frequency dielectric constant, n is the conduction-electron concentration, and under the assumed conditions,

$$k^2 = 3\kappa T m^* / \hbar^2 \quad (9)$$

Therefore, gamma is given by

$$\begin{aligned}\gamma^2 &= 4k^2 / \beta^2 \\ &= 12e^2nm^*/\epsilon_0K\hbar^2\end{aligned}\tag{10}$$

Notice that gamma is explicitly independent of temperature, but temperature in combination with n must be considered in order to determine whether the electron system is non-degenerate, as assumed.

For example, suppose $m^* = 0.2m$ and $K = 10$. If the electron concentration is $n = 1 \times 10^{15}/cc$, then gamma squared is equal to 5.7×10^{31} and the second term in eq. (7) is relatively very small and nearly equal to unity. Therefore, the BH and FC models give quite similar results, since the second term is almost negligible (unity) in comparison to the logarithm term (7). Hence, there is essentially no difference between the BH and FC scattering models within about 2%.

However, if $n = 1 \times 10^{22}/cc$, a full-blown calculation including degeneracy and a nonparabolic conduction band gives gamma squared equal to 5.35; the logarithm term is 1.85 and the second term is 0.84. In this case, there is quite a large difference between the BH and FC models, *i.e.* 166%. More-detailed comparisons are given in the following section.

1.6 Comparisons between BH and FC Theories

Figure 11 shows the comparison between BH and FC theories calculated by SETA for 300K GaAs. The SETA calculations use the parameters given in the Appendix. The compensating acceptors are important only for low electron concentrations. The acceptor concentration is arbitrarily set at a fixed $3.1 \times 10^{15}/cc$ but the actual value is not known for each experimental datum. Our interest is primarily in the high-concentration region of the figure. Clearly, the BH theory is much too high and the FC theory is much too low for heavily doped material. BH is about 60% too high and FC is about 40% too low — well beyond our desired 5% criterion. Of course, agreement could be forced by arbitrarily adjusting the compensating acceptor concentration, but this approach would contradict experimental evidence that acceptors play very little role in these materials, *i.e.* photoluminescence shows no acceptors in Sn-doped GaAs, and group VI donors such as S and Te cannot yield acceptor behavior under these conditions.

Naturally, one wonders what might result at 77K. This comparison is shown in Figure 12 where FC is seen to sometimes agree and at other times disagree with BH entirely.

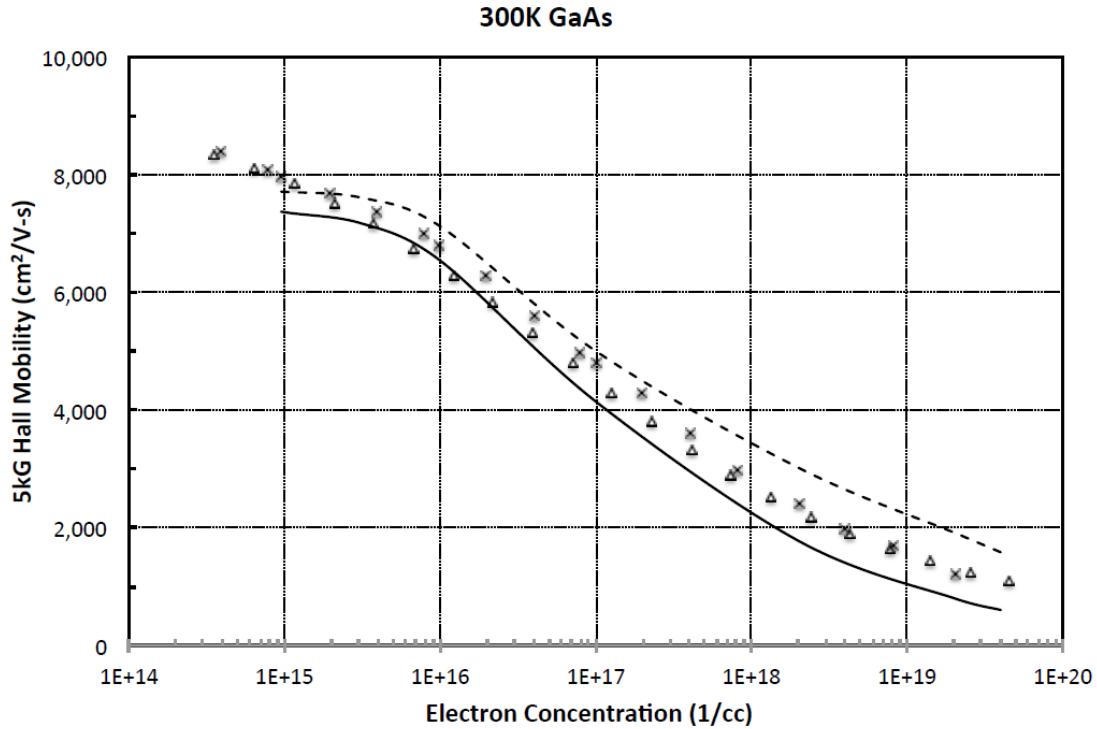


Figure 11: 300K Electron Mobility of Doped GaAs Compiled by Sotoodeh⁸ and by Stillman⁹ et al.
 Compared to BH theory (dashed curve) and FC theory (solid curve).

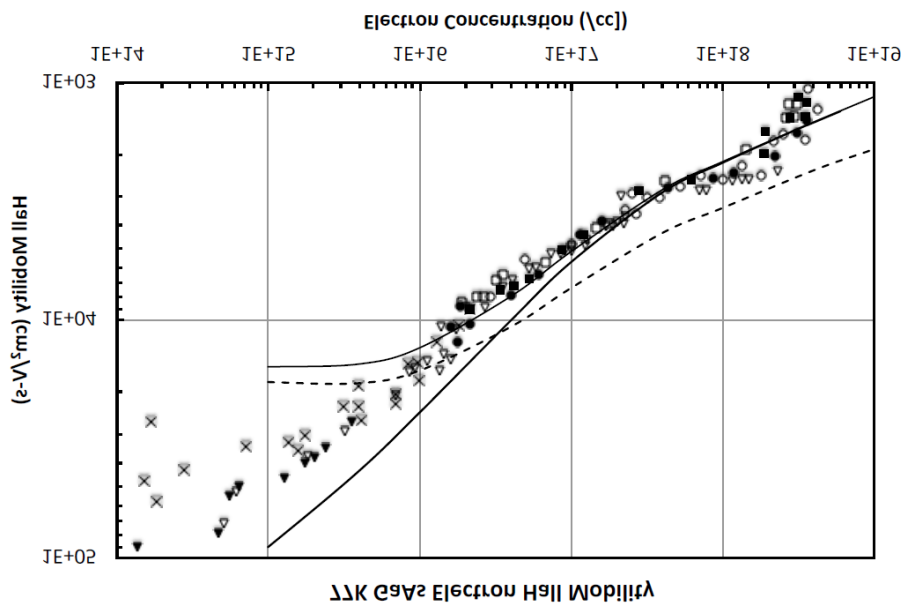


Figure 12: 77K Electron Mobility of Doped GaAs by Balk¹⁰ and by Kuphal¹¹
 Compared to BH Theory (dashed curve) and FC Theory (solid curves)
 The FC case, acceptor concentrations are zero and $5 \times 10^{15}/\text{cc}$. For the FC case, acceptor concentration is $5 \times 10^{15}/\text{cc}$.

2 CONCLUSION

Results shown in Figures 8, 9, 11 and 12 for InP and GaAs show clearly that it is not possible to force agreement between theory and experiment to within a few percent, given that arbitrary assumptions about acceptor compensation are not admissible.

Furthermore, the work by Falicov and Cuevas raises an interesting question regarding spatial correlation between dopants and its effect on electron scattering, which is not considered in the Brooks-Herring theory. This effect seems to be especially important at high doping levels.

However, FC presumes that the spatial correlation occurs between acceptor and donor species, which produces a conundrum if acceptors are not allowed and, hence, there are no acceptors!

A partial resolution of this paradox is developed in Phase 2 of this work.

3 ACKNOWLEDGMENTS

Supported by the Air Force Office of Scientific Research under Project FA9550-20RXCOR046-RY. This work would not have been possible without encouragement and advice from John S. Cetnar. It is a pleasure to acknowledge helpful suggestions and discussions with David C. Look.

APPENDIX

Material parameters used for 300K SETA calculations are as follows. GaAs:

low-frequency dielectric constant 12.91

high-frequency dielectric constant 10.91 optical phonon temperature 419K elastic constant 1.4×10^{11} N/m² deformation potential 8.6 eV piezoelectric coefficient 0.052

energy gap 1.54 eV effective mass 0.066m

InP:

low-frequency dielectric constant 12.38 high-frequency dielectric constant 9.55 optical phonon temperature 497K elastic constant 1.21×10^{11} N/m² deformation potential 6.8 eV piezoelectric coefficient 0.0131

energy gap 1.42 eV effective mass 0.082m

4 REFERENCES

1. Lest one be tempted to overlook the importance of semiconductor science and technology with regard to defensive and competitive ability, note the following from China (PRC). Source: Global Times 2020/10/24 16:13:47: (emphasis added)
“Technologies relevant to *semiconductors*, 5G and quantum computing, among others will be likely mentioned in the 14th Five-Year Plan. Policy support involving taxes support and talent nurturing will surely be included,” Li Chang'an, a professor at the University of International Business and Economics' School of Public Administration, told the Global Times on Friday.
2. D. L. Rode, *Semiconductors and Semimetals* **15** (Academic Press, New York, 1975) Ch. 1.
3. D. L. Rode and P. Fedders, *J. Appl. Phys.* **54** (1983) 6425.
4. H. Brooks, *Advan. Electron. Electron Phys.* **7** (1955) 85, and C. Herring, unpublished.
5. L. M. Falicov and M. Cuevas, *Phys. Rev.* **164** (1967) 1025.
The GaAs sample was grown using (Vapor Phase Epitaxy) VPE, by T. H. Meiers (Motorola, Semiconductor Research & Development Labs). Hall measurements were carried out at McDonnell-Douglas Research Labs (data points). SETA calculations are by
D. L. Rode. (curve).
6. There is necessarily some degree of arbitrariness in specifying what one means by the qualifier “accurate.” Here, the objective is to achieve 5% accuracy, based on the following experience. In the 1990’s, during an aggressive development phase of GaAs for gigahertz electronics applications, the author was involved with a round-robin project headed by NIST to determine the state-of-the-art of the accuracy of Hall Effect measurements in the industry. Some 12 different commercial R&D labs were involved, as well as exceedingly careful measurements by NIST. Approximately 20 different epitaxial wafers were selected, laser scribed with labeling on the backside by Cutting Edge Optronics, diamond sawn into 10mm squares by D. L. Rode, and blind distributed to various labs for 300K and 77K Hall measurements. When the results were collected at NIST, it was surprising to find that there was a large amount of scatter in the results, with variations reaching up to about 12 percent! Reproducibility was checked and found not to be a significant source of error. On average, after rejecting the worst outliers, the standard deviation was still about 7 percent. We concluded that the state-of-the-art in accuracy is perhaps as good as 5 percent. The author feels that the probable largest source of error is related to the magnetic field, both in determining its magnitude and in being sure that it is transverse to the electrical current flow. There may also be a problem with ohmic contacts, but the project was abandoned before this could be examined further. To help further the standardization of Hall Effect measurements, the present author wrote the procedure given in the NIST www site: <https://www.nist.gov/>. Search for Hall Effect.
7. M. Sotoodeh, A. H. Khalid, and A. A. Rezazadeh, *J. Appl. Phys.* **87** (2000) 2890.

8. M. R. Borzel and G. E. Stillman, *Properties of Gallium Arsenide*, (INSPEC, London, 1996) p. 106.
9. E. Veuhoff, M. Maier, K.-H. Bachem, and P. Balk, *J. Crystal Growth* **53** (1981) 598.
10. E. Kuphal, *J. Crystal Growth* **54** (1981) 117.
11. D. A. Anderson and N. Apsley, *J. Appl. Phys.* **58** (1985) 3059.
12. W. Walukiewicz et al., *J. Appl. Phys.* **51** (1980) 2659.
13. B. Fischer, E. Bauser, P. A. Sullivan, and D. L. Rode, *Appl. Phys. Letters* **33** (1978) 78.

LIST OF SYMBOLS, ABBREVIATIONS, AND ACRONYMS

ACRONYM	DESCRIPTION
AFRL	Air Force Research Laboratory
BH	Brooks-Herring
Eq	Equation
FC	Falicov-Cuevas
GaAs	Gallium Arsenide
GaN	Gallium Nitride
GZO	Gallium Zinc Oxide
LPE	Liquid Phase Epitaxy
SETA	Semiconductor Electronic Transport Analysis
Te	Tellurium
VPE	Vapor Phase Epitaxy